

# New Skills or Sharper Primitives? A Probabilistic Perspective on the Emergence of Reasoning in RLVR

Zhilin Wang<sup>1,2</sup> Yafu Li<sup>2,3</sup> Shunkai Zhang<sup>4</sup> Zhi Wang<sup>5</sup> Xiaoye Qu<sup>2</sup> Haoran Zhang<sup>2,6</sup> Yu Cheng<sup>3</sup>

## Abstract

Whether Reinforcement Learning with Verifiable Rewards (RLVR) endows Large Language Models (LLMs) with new capabilities or merely elicits latent traces remains a central debate. In this work, we align with the former view, proposing a probabilistic framework where capability is defined by instance-level solvability. We hypothesize that the emergence of complex reasoning can be driven by sharpening atomic step probabilities, which enables models to overcome the exponential decay of success rates inherent in multi-step reasoning chains. Utilizing the Algebrarium framework, we train models exclusively on single-step operations and evaluate their performance on unseen multi-step tasks. Our empirical results confirm that: (1) RLVR incentivizes the exploration of previously inaccessible solution paths by amplifying the model’s existing skills; (2) composite performance is strictly governed by the joint probability of atomic steps, evidenced by high Pearson correlation coefficients ( $\rho \in [0.69, 0.96]$ ); and (3) RLVR, acting as a global optimizer, can cause specific skills to be sacrificed to maximize aggregate reward. Our work offers a novel explanation for emergent abilities in RLVR, suggesting that the iterative optimization of solvable problems enables models to develop the capabilities to tackle previously unsolvable scenarios.

## 1. Introduction

While the Reinforcement Learning with Verifiable Rewards (RLVR, Shao et al., 2024) paradigm has achieved impressive success (OpenAI et al., 2019; DeepMind, 2025), a cen-

<sup>1</sup>University of Science and Technology of China <sup>2</sup>Shanghai AI Laboratory <sup>3</sup>The Chinese University of Hong Kong <sup>4</sup>Peking University <sup>5</sup>Nanjing University <sup>6</sup>Shanghai Jiao Tong University. Correspondence to: Yafu Li <yafuly@gmail.com>, Yu Cheng <chengyu@cse.cuhk.edu.hk>.

tral question is whether it endows Large Language Models (LLMs) with genuinely new capabilities or merely elicits traces already latent within the models themselves. This question stands at the forefront of current research. Some studies argue for the former, positing that RLVR implants new compositional skills absent in the base model (Yuan et al., 2025; Cheng et al., 2025); conversely, other works maintain the latter, suggesting that RLVR acts primarily as a mechanism to unlock pre-existing potentials (Yue et al., 2025; Gandhi et al., 2025; Liu et al., 2025; Zhao et al., 2025).

In this work, we align with the former perspective, anchoring our argument in a rigorous probabilistic definition of capability: if a model fails to produce a solution despite exhaustive sampling, it is fundamentally devoid of the corresponding capability. Such complex problems often necessitate sequential reasoning, where success hinges on the correctness of each intermediate step (Wei et al., 2023). While the base model may possess the competence to solve individual atomic steps, the cumulative probability of executing a perfect chain is negligible, rendering the complex task practically unsolvable (Dziri et al., 2023). By significantly improving the accuracy of each individual step, RLVR prevents errors from accumulating in long chains. This allows the model to reliably complete complex reasoning paths that were previously too unlikely to succeed. Thus, while RLVR may not impart novel knowledge (Zhou et al., 2023), it nonetheless unlocks a genuinely new capability through reliable composition.

Our work begins with a comprehensive theoretical analysis of *Pass@k* across the entire dataset, decomposing aggregate metrics to extract the specific success rate for each individual problem. We propose using this instance-level solvability as the intrinsic measure of capability. By scrutinizing the success rates of complex tasks, we uncover a theoretical bottleneck: the *Multiplicative Barrier*. We demonstrate that the vanishing solvability for reasoning-heavy problems is a mathematically inevitable consequence of exponential decay, where the joint probability of a solution collapses as the product of atomic step probabilities. Consequently, we frame RLVR-induced emergence as a phase transition where the sharpening of atomic probabilities enables the

model to pierce through this multiplicative ceiling. Furthermore, we characterize *Capability Erosion* as a side effect of optimizing for expected utility. Since the RLVR objective optimizes from a global distributional perspective, the resulting gradient updates do not inherently preserve instance-level stability, potentially leading to performance degradation on specific instances.

To rigorously validate these theoretical assumptions, we conduct a controlled experimental study using the Algebrarium framework. We design a strict “Atomic-Composite Split” protocol to isolate the mechanism of emergence: models are trained exclusively on decoupled atomic primitives but evaluated on their ability to solve unseen composite problems. Our empirical analysis yields four critical insights into the nature of capability emergence:

- **Validation of  $\text{Pass}@k$  Dynamics:** We derive  $\text{Pass}@k$  as an explicit function of per-instance correctness probabilities and show that the resulting curves closely match empirical measurements.
- **Operational definition of emergence:** Using instance-level solvability thresholds, we visualize a phase transition in which RLVR moves problems from the **Null Set** to the **Feasible Set**.
- **Mechanism via the multiplicative barrier:** We verify that multi-step reasoning success decays exponentially with reasoning depth ( $P \propto p^N$ ) and that composite performance is strongly predicted by the joint probability of atomic steps (Pearson  $\rho \in [0.69, 0.96]$ ).
- **Trade-off via capability erosion:** We document that optimizing expected reward can improve aggregate performance while degrading specific (including atomic) instances, highlighting a redistribution of capability rather than uniform gains.

In conclusion, our work offers a novel explanation for emergent abilities in RLVR, suggesting that the iterative optimization of solvable problems enables models to develop the capabilities to tackle previously unsolvable scenarios.

## 2. Related Work

**Reinforcement Learning with Verifiable Rewards (RLVR).** The RLVR paradigm has become pivotal for enhancing LLM reasoning abilities (OpenAI, 2024; DeepMind, 2025). These algorithms update the policy based on the relative advantage of sampled paths, reinforcing trajectories that outperform the group advantage (DeepSeek-AI et al., 2025; Shao et al., 2024; Yu et al., 2025; Zheng et al., 2025). However, the efficacy of this sampling-based optimization has sparked a fundamental debate: does this

process merely surface latent traces, or does it genuinely endow the model with new capabilities (Yue et al., 2025)?

**Perspective I: RLVR merely elicits latent traces.** A growing body of research suggests that RLVR amplifies existing competencies rather than injecting new capabilities (Zhao et al., 2025; Wen et al., 2025). Empirically, RLVR training is observed to reduce entropy (Cui et al., 2025; Wang et al., 2025; Jiang et al., 2025; Yan et al., 2025) and often degrade  $\text{Pass}@k$  performance compared to baselines, indicating a contraction of exploration space rather than capability expansion (Yue et al., 2025; Zhu et al., 2025; He et al., 2025). Theoretically, this limitation stems from the dependence of on-policy algorithms on spontaneous generation: if a correct solution cannot be sampled, the model receives no reward signals (Zhan et al., 2025). Thus, RLVR is viewed merely as a mechanism to elicit latent potentials already encoded during pre-training.

**Perspective II: RLVR implants new capabilities.** Conversely, some recent studies challenge the elicitation hypothesis, arguing that RLVR can induce novel, complex composite capabilities (Yuan et al., 2025; Cheng et al., 2025). To control for confounding environmental factors, researchers employ synthetic tasks such as the Countdown problem or design specific environments to disentangle atomic skills from composite reasoning (Park et al., 2025). Contrary to the first perspective, these works observe a substantial improvement in  $\text{Pass}@k$  after training, suggesting that RLVR facilitates the induction of novel reasoning paths rather than the mere elicitation of latent ones. However, the underlying mechanism driving this emergence remains underexplored.

Our work provides both theoretical and experimental support for the second perspective, demonstrating that RLVR induces novel capabilities by optimizing solvable atomic sub-tasks to construct complex reasoning paths previously absent from the base model.

## 3. Understanding the $\text{Pass}@k$ Curve

### 3.1. Theoretical Analysis

Given a dataset  $\mathcal{D} = \{q_i\}_{i=1}^N$  consisting of  $N$  problems, the  $\text{Pass}@k$  metric measures the proportion of problems successfully solved by at least one solution when  $k$  candidate solutions are generated per problem:

$$\text{Pass}@k = \frac{1}{|\mathcal{D}|} \sum_{i=1}^{|\mathcal{D}|} \mathbb{I}(\text{solved}_i \geq 1), \quad (1)$$

where  $\mathbb{I}(\cdot)$  is the indicator function, and  $\text{solved}_i \in \{0, 1, \dots, k\}$  represents the count of successful samples for the  $i$ -th problem out of  $k$  independent generations.

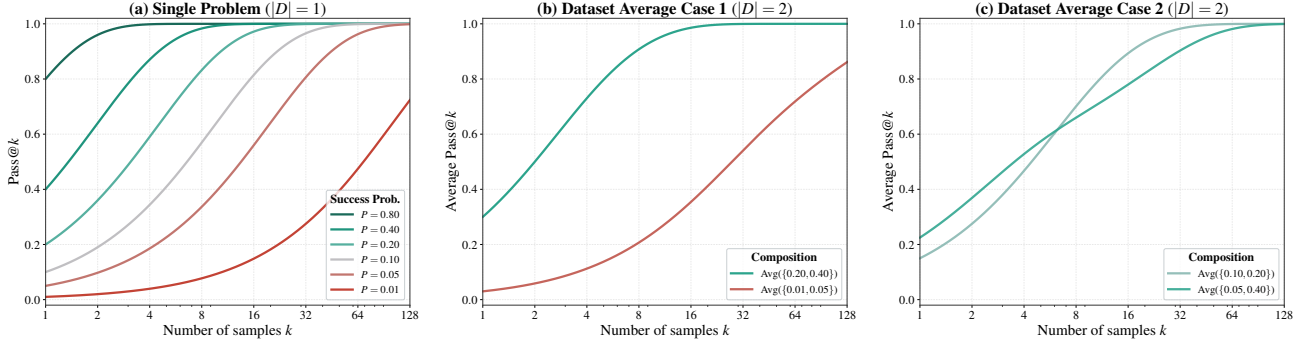


Figure 1. Theoretical visualization of  $Pass@k$ . (a) Functional curves for a single problem under varying correctness probabilities. (b) and (c) Composite average curves for a simplified dataset ( $|\mathcal{D}| = 2$ ), showing the aggregation from instances to the dataset-level metric.

To formalize this, let  $\pi_\theta(y|q)$  denote the policy of the model generating a solution  $y$  for a query  $q \in \mathcal{Q}$ . Let  $V(y, q) \in \{0, 1\}$  be the correctness verification function. The success probability for a specific task  $q$  is defined as the expectation of correctness over the model's generation distribution:

$$P_\theta(q) = \mathbb{E}_{y \sim \pi_\theta(\cdot|q)} [V(y, q)] \quad (2)$$

First, consider a single problem  $q$ . Assuming  $k$  samples are generated independently, the probability that all  $k$  samples fail is  $(1 - P_\theta(q))^k$ . Consequently, the expected  $Pass@k$  for this single instance is:

$$E[Pass@k(q)] = 1 - (1 - P_\theta(q))^k \quad (3)$$

Generalizing this to the entire dataset  $\mathcal{D}$ , the overall  $pass@k$  is defined as the arithmetic mean of the expected pass rates across all  $N$  instances:

$$E[Pass@k] = \frac{1}{N} \sum_{i=1}^N [1 - (1 - P_\theta(q_i))^k] \quad (4)$$

By analyzing the behavior of the  $Pass@k$  metric, we can disentangle distinct dimensions of model performance.

### 3.2. From Theory to Estimation

To intuitively illustrate this theoretical framework, Figure 1 presents two complementary views. Figure 1(a) plots the functional curves for a single problem under varying correctness probabilities, demonstrating how the curve's shape is strictly determined by the specific correctness rate. In contrast, Figure 1(b) and (c) consider simplified datasets where  $|\mathcal{D}| = 2$ . They visualize the composite average curve formed by aggregating two distinct problem instances, highlighting the theoretical composition process from individual problems to the dataset-level metric.

**Post-RLVR Degradation in High- $k$  Sampling.** The phenomenon of decreasing  $Pass@k$  after RLVR, as noted in prior work (Yue et al., 2025), can be explained using Figure 1. Specifically, post-RLVR models in their work tend to increase  $Pass@k$  at low  $k$  values while decreasing it at high  $k$ . This suggests that RLVR polarizes their model's success probabilities across the task distribution. It drives the correctness probability of certain problems towards certainty, while inadvertently reducing the probability of solving others. Consequently, this polarization improves  $Pass@1$ , but harms the broader coverage measured by high- $k$  metrics.

## 4. Capability as Probabilistic States

To rigorously quantify model capability, we move beyond aggregate metrics and analyze the pointwise convergence of  $P_\theta(q)$ . We posit that for a given model  $\pi_\theta$ , the task space  $\mathcal{Q}$  can be partitioned based on the solvability of tasks under a computational budget constraint.

Based on the magnitude of  $P_\theta(q)$ , we partition the task space  $\mathcal{Q}$  into distinct capability regions. We introduce two critical thresholds: an infinitesimal bound  $\epsilon \rightarrow 0^+$  representing statistical impossibility, and a feasibility lower bound  $\delta \in (0, 1]$  representing reliable solvability.

**Definition 1: The Null Set ( $\epsilon$ -Incapability).** A task  $q$  belongs to the *Null Set*  $\mathcal{N}_\theta^\epsilon$  if the probability of generating a correct solution is asymptotically negligible. This state represents a topological disconnection between the problem and the model's reachable hypothesis space. Formally:

$$\mathcal{N}_\theta^\epsilon = \{q \in \mathcal{Q} \mid P_\theta(q) < \epsilon\} \quad (5)$$

Empirically, we determine  $\epsilon$  using the statistical *Rule of Three*. If zero successes are observed in a large-sample regime (e.g.,  $K_{\text{large}} = 128$ ), the upper bound of the 95% confidence interval for the true success rate is approximately  $3/K_{\text{large}}$ . Thus, we set  $\epsilon \approx 0.023$ . A task in this set implies

that correctness is effectively a zero-probability event under the current model parameters.

**Definition 2: The Feasible Set ( $\delta$ -Capability).** Conversely, a task is considered *Feasible* if the success probability is bounded away from zero by a sufficient margin  $\delta$ . This ensures that the task can be solved reliably within a finite compute budget. We define the Feasible Set  $\mathcal{F}_\theta^\delta$  as:

$$\mathcal{F}_\theta^\delta = \{q \in \mathcal{Q} \mid P_\theta(q) \geq \delta\} \quad (6)$$

Here,  $\delta$  is calibrated to a minimum compute budget  $K_{\min}$  (e.g., standard parallel inference where  $K_{\min} = 8$ ). By setting  $\delta = 1/K_{\min} = 0.125$ , we guarantee that the expected number of correct solutions is at least 1:

$$K_{\min} \cdot P_\theta(q) \geq 1 \quad (7)$$

This condition distinguishes stable capability from stochastic outliers (“lucky guesses”), ensuring that the model possesses the intrinsic features required to solve  $q$ .

**The Stochastic Gap.** Tasks falling in the interval  $\mathcal{Q} \setminus (\mathcal{N}_\theta^\epsilon \cup \mathcal{F}_\theta^\delta)$ , where  $\epsilon \leq P_\theta(q) < \delta$ , are classified as *Transitional States*. These tasks exhibit high variance and represent the frontier of the model’s learning process. For the purpose of robust capability analysis, we focus our subsequent discussion on the phase transition between the limit of impossibility ( $\mathcal{N}_\theta^\epsilon$ ) and the state of reliable capability ( $\mathcal{F}_\theta^\delta$ ).

## 5. Gain and Loss of Capability

In this section, we analyze the dual impact of RLVR optimization on model capabilities, exploring two simultaneous phenomena driven by the model’s finite capacity. First, we define *Compositional Emergence*, illustrating how the linear amplification of atomic steps triggers a geometric phase transition, rendering previously intractable complex tasks solvable. Then, we examine *Capability Erosion*, demonstrating that RLVR optimization for global rewards can inadvertently degrade specific skills.

### 5.1. The Multiplicative Barrier in Complex Reasoning

Consider a complex problem  $q$  that can be decomposed into a sequence of  $M$  sub-problems, denoted as  $\mathcal{S} = \{s_1, s_2, \dots, s_M\}$ . For the model to successfully solve  $q$ , it must correctly execute each sub-problem  $s_j$  in the chain.

Under the assumption that the correctness of each step is independent, the overall success probability  $P_\theta(q)$  is the product of the success probabilities of the individual sub-problems:

$$P_\theta(q) \approx \prod_{j=1}^M P_\theta(s_j) \quad (8)$$

This multiplicative nature creates a severe barrier for deep reasoning. Even if the model exhibits reliable capability for every atomic sub-problem (e.g.,  $P_\theta(s_j) = 0.3$ ), the joint probability decays exponentially with the chain length  $M$ .

For a problem requiring  $M = 5$  such steps, the cumulative success rate collapses to:

$$P_\theta(q) \approx 0.3^5 \approx 0.0024$$

Crucially, this value falls an order of magnitude below the statistical existence threshold  $\epsilon \approx 0.023$  (the Null Set boundary). Then, while the model is locally capable of every step, it appears globally incapable of solving the whole problem  $q$ . Empirically, this results in zero successes ( $\text{Pass}@128 = 0$ ), masking the model’s underlying potential.

### 5.2. Emergence through Probability Amplification

RL can operate by optimizing these atomic primitives where reward signals are dense. By sufficiently “sharpening” the atomic probabilities, RLVR triggers a multiplicative phase transition at the compositional level. We formalize this emergence as the crossing of the feasibility boundary:

$$\underbrace{0.3^5 \approx 0.0024}_{\text{Null State } (P_\theta(q) < \epsilon)} \xrightarrow[\text{Sharpening}]{\text{RL}} \underbrace{0.7^5 \approx 0.168}_{\text{Feasible State } (P_\theta(q) \geq \delta)}$$

Here, the new capability to solve  $Q_{\text{comp}}$  emerges not from learning the complex task logic directly, but from the saturation of prerequisite atomic competencies. This resolves the central paradox: RLVR acts as an amplifier at the micro-level, which mathematically necessitates its appearance as a creator at the macro-level.

### 5.3. Capability Erosion under RLVR Optimization

While RLVR acts as an amplifier for emergence, this optimization is not a monotonic improvement across the entire task domain. Instead, it often triggers *Capability Erosion*, a phenomenon where the mastery of certain problem instances comes at the expense of others.

The RLVR objective is defined by the maximization of the expected reward over the task distribution  $\mathcal{D}$ :

$$\max_{\theta} \mathcal{J}(\theta) = \frac{1}{N} \sum_{i=1}^N \mathbb{E}_{x \sim \pi_\theta(\cdot | q_i)} [R(x)] \quad (9)$$

By maximizing mean reward, RLVR prioritizes the majority over the specific. This creates an inherent conflict: to master dominant tasks, the model may overwrite representations required for minority cases. As a result, training does not yield a uniform improvement; rather, it triggers a redistributive trade-off. Ultimately, the erosion of minority skills is the price of global improvement, showing that RL reshapes through destruction rather than simple accumulation.

**Table 1. Dataset Statistics and Domain Properties.** We evaluate four algebraic systems varying in cardinality and commutativity. The training set consists exclusively of atomic examples to enforce rule learning, while the test set comprises 800 samples stratified by reasoning depth (2–5 operations) to assess generalization.

Domain	Group Properties		Underlying Structure	Train	Test (Stratified by Depth)					Total
	Card.	Comm.			1-Ops	2-Ops	3-Ops	4-Ops	5-Ops	
Encrypted History	$\infty$	Yes	Integers ( $\mathbb{Z}$ )	3,200	50	50	50	50	200	200
Enigma System	Finite	Yes	Modular Product ( $\mathbb{Z}_{26}^3$ )	3,200	50	50	50	50	200	200
Knitting System	$\infty$	No	Free Group	3,200	50	50	50	50	200	200
Rubik’s Cube	Finite	No	Permutation Group	3,200	50	50	50	50	200	200
<b>Total</b>	<i>4 Distinct Algebraic Systems</i>				<b>12,800</b>	<b>200</b>	<b>200</b>	<b>200</b>	<b>200</b>	<b>800</b>

## 6. Experiment Setup

To isolate genuine logical deduction from memorized knowledge, we employ Algebraarium to generate synthetic symbolic reasoning tasks. This framework mitigates contamination by instantiating non-standard algebraic structures that do not exist in pre-training corpora. It provides a clean environment characterized by tunable complexity, deterministic answers, and a modular design that makes the reasoning process highly analyzable. By decoupling abstract definitions from concrete instances, Algebraarium ensures that performance reflects pure symbolic proficiency rather than data leakage. (Detailed in Appendix A.)

**Domains and Task Formulation.** The core task is *Algebraic Expression Calculation*. Given two elements  $e_1, e_2 \in G$  from a specific group, the model must compute the canonical result of  $e_1 \oplus e_2$  by applying group axioms (e.g., associativity, identity, inverse). To test robustness across diverse algebraic properties, we configure four distinct domains defined by two axes: Cardinality (Finite vs. Infinite) and Commutativity (Abelian vs. Non-Abelian).

**Table 2. Evaluation Framework.** The framework distinguishes between direct inference and decomposed binary operations. Note that all intermediate steps  $d_j$  are defined as ground truth labels to allow for independent assessment of atomic operations ( $P_\theta(s_j)$ ).

Mode	Structure (Binary Ops)	Metric
Direct	$q \xrightarrow{\text{Infer}} \text{Result}$	$P_\theta(q)$
Decomposed	<i>Sequential Chain</i>	
Step 1	$s_1 : e_1 \oplus e_2 \rightarrow d_1$	$P_\theta(s_1)$
...	...	...
Step $j$	$s_j : e_k \oplus d_{j-1} \rightarrow d_j$	$P_\theta(s_j)$
Step $N$	$s_N : e_{final} \oplus d_{N-1} \rightarrow \text{Res}$	$P_\theta(s_N)$
Definitions	<ul style="list-style-type: none"> <li>• <b>Atomic:</b> <math>P_\theta(s_j)</math></li> <li>• <b>Result:</b> <math>P_\theta(q)</math></li> <li>• <b>Joint:</b> <math>\prod_{j=1}^N P_\theta(s_j)</math></li> </ul>	

**Measurement and Decomposition.** As shown in Table 2, We quantify difficulty by operation count  $N$  and compare direct inference  $P_\theta(q)$  with decomposed binary steps  $s_j$ .

Our analysis relates instance accuracy  $P_\theta(q)$  to atomic step accuracy  $P_\theta(s_j)$  and the joint probability  $\prod_{j=1}^N P_\theta(s_j)$ .

**Dataset Construction.** Our data split is designed to decouple rule acquisition from compositional reasoning.

- **Training:** The training set is strictly limited to *atomic* operations (1-hop reasoning). This forces the model to internalize the fundamental axioms of each group.
- **Testing:** The test set evaluates the model’s ability to chain these axioms. It is stratified into four difficulty levels based on operation depth (2 to 5 ops), with 200 balanced samples per level across all domains.

Table 1 summarizes our dataset configuration. Further details for each task are provided in Appendix C.

**Implementation Details.** We benchmark three model families: LLAMA, QWEN, and GEMMA. Training employs Group Relative Policy Optimization (GRPO, Shao et al., 2024) for 100 steps. Performance is measured via exact match accuracy of the final boxed output. Further details are provided in Appendix B.

## 7. Empirical Validation of the Theory

To validate the theory in Section 3.1, we evaluate LLAMA, QWEN, and GEMMA models across several dimensions. Our experiments trace a causal chain from *Pass@k Curve Dynamics* to the *Multiplicative Barrier* of complex reasoning, showing how these drive *Compositional Emergence* and, ultimately, *Capability Erosion*.

### 7.1. Validation of Theoretical *Pass@k* Dynamics

First, we examine the fidelity of our theoretical model in capturing the empirical behavior of the *Pass@k* metric. To construct the theoretical curves, we necessitate an estimate of the intrinsic correctness probability  $P_\theta(q)$  for each problem. We approximate this parameter by computing the av-

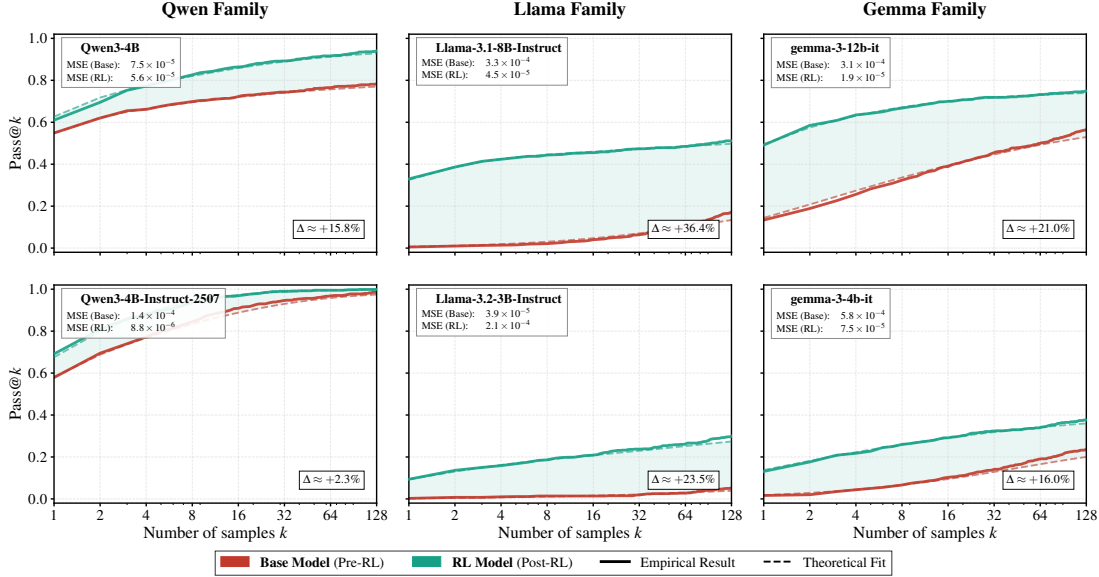


**Figure 2. Comparison of theoretical and empirical  $\text{Pass}@k$  curves.** The figure illustrates that the theoretical and empirical curves align remarkably well, consistently yielding a Mean Squared Error (MSE) magnitude less than  $10^{-4}$ . Furthermore, the RL models demonstrate substantial performance improvements over the Base models across the sampling spectrum.

verage correctness rate over 128 sampled responses for each instance (i.e.,  $P_\theta(q) \approx \text{Avg}@128(Q)$ , using Eq. 2). The comparison between these theoretically projected curves and the actual empirical results is presented in Figure 2.

As shown in Figure 2, empirical results align with our theory with high precision, confirming the Section 3.1 formulation. Significant improvements in  $\text{Pass}@k$  suggest that RLVR enables the model to solve previously intractable problems, signaling the emergence of new capabilities.

## 7.2. Transitions from the Null Regime

Building on the probabilistic definitions established in Section 4, we investigate the mechanism of emergence. We rigorously isolate the subset of tasks initially classified within *The Null Set* for the base models. To ensure evaluation robustness, we define the acquisition of capability strictly as the transition into *The Feasible Set*.

As illustrated in Figure 3, RLVR effectively unlocks 22.6% of tasks from the Null Set, elevating the mean success rate of this activated subset from 0 to 0.60. This shift substantiates that emergence arises when optimized atomic probabilities surmount the multiplicative barrier, rendering previously intractable tasks reliably solvable.

## 7.3. Validating the Multiplicative Barrier Hypothesis

Section 5 attributes the difficulty of complex tasks to the exponential decay of joint probabilities ( $\prod P_\theta(s_j)$ ). We empirically validate this *Multiplicative Barrier* empirically

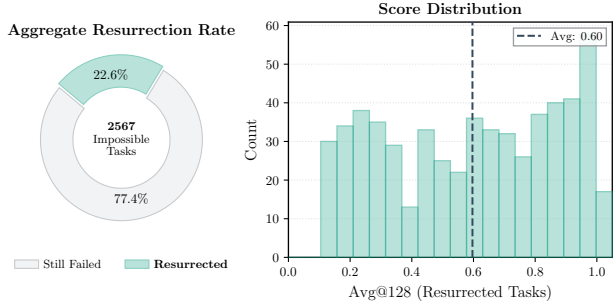


**Figure 3. Analysis of Capability Emergence.** We analyze the subset of tasks initially classified as Null State ( $\text{Avg}@128 = 0$ ) in the Base model. **Left:** The recovery rate, indicating the proportion of these impossible tasks that successfully transitioned to the Feasible State ( $\text{Avg}@128 \geq 0.125$ ) after RL training. **Right:** Post-emergence accuracy distribution. The significant skew toward high performance (mean  $\approx 0.60$ ) indicates that emergence occurs as a sharp phase transition.

through two complementary analyses.

**Existence of the Exponential Barrier.** Figure 4 delineates a distinct performance boundary, effectively acting as a “soft wall” for model capabilities. We observe that accuracy undergoes a geometric decay relative to task complexity, closely following the function  $y \approx p^x$ . This trajectory provides empirical confirmation that reasoning errors accumulate multiplicatively: the joint probability of success

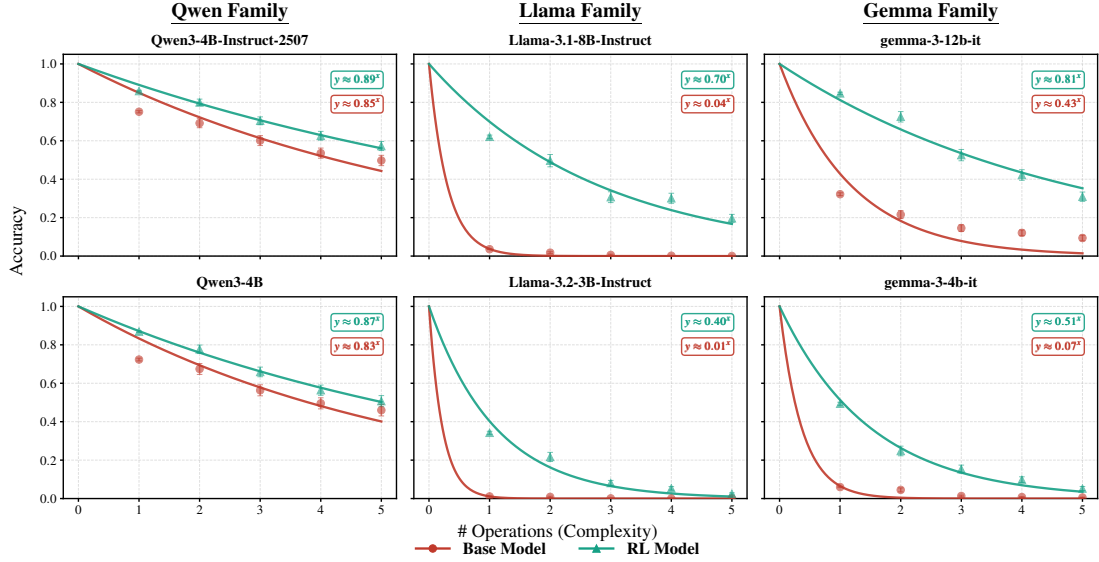


Figure 4. Verification of Exponential Decay. The figure validates the *Multiplicative Barrier* hypothesis ( $P \propto p^N$ ).

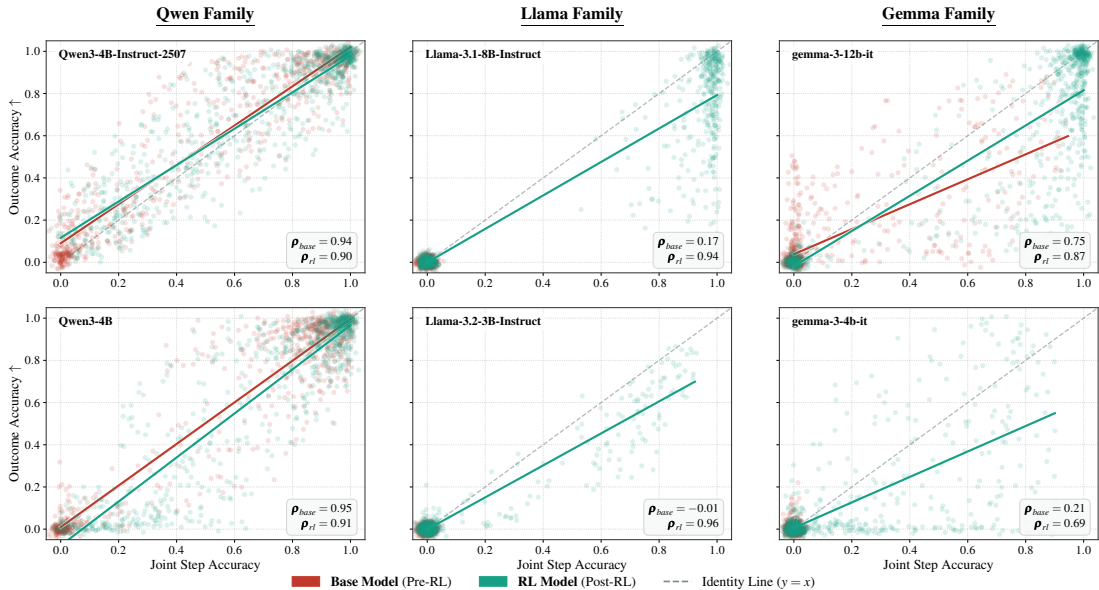


Figure 5. Process vs. Outcome Correlation Analysis. Scatter plots correlating joint step accuracy ( $\prod P_\theta(s_j)$ ) with Outcome Accuracy ( $\prod P_\theta(q)$ ). Selected base models from the Llama and Gemma families cluster in the “Null Regime” near the origin, indicating that a breakdown in the joint reasoning chain leads to task failure. In contrast, Qwen models and RL-tuned models exhibit a high correlation.

is the product of individual atomic probabilities. Consequently, even with high atomic accuracy, the likelihood of a correct final outcome diminishes exponentially as the reasoning horizon extends, rendering highly complex tasks rapidly intractable.

**Correlation as the Mechanism of Emergence.** To uncover the mechanism behind the “Zero-to-One” emergence phenomenon observed in Section 7.2, Figure 5 analyzes the

correlation between joint step accuracy and final answer correctness. The data reveal that the emergence of complex capabilities is structurally bound by this correlation.

Prior to RLVR, Gemma and Llama models exhibit a “broken link” between process and outcome, clustering near the origin. Without sufficient atomic accuracy, the probabilistic chain collapses, preventing the capability from manifesting.

The transition to RLVR restores the linear coupling between

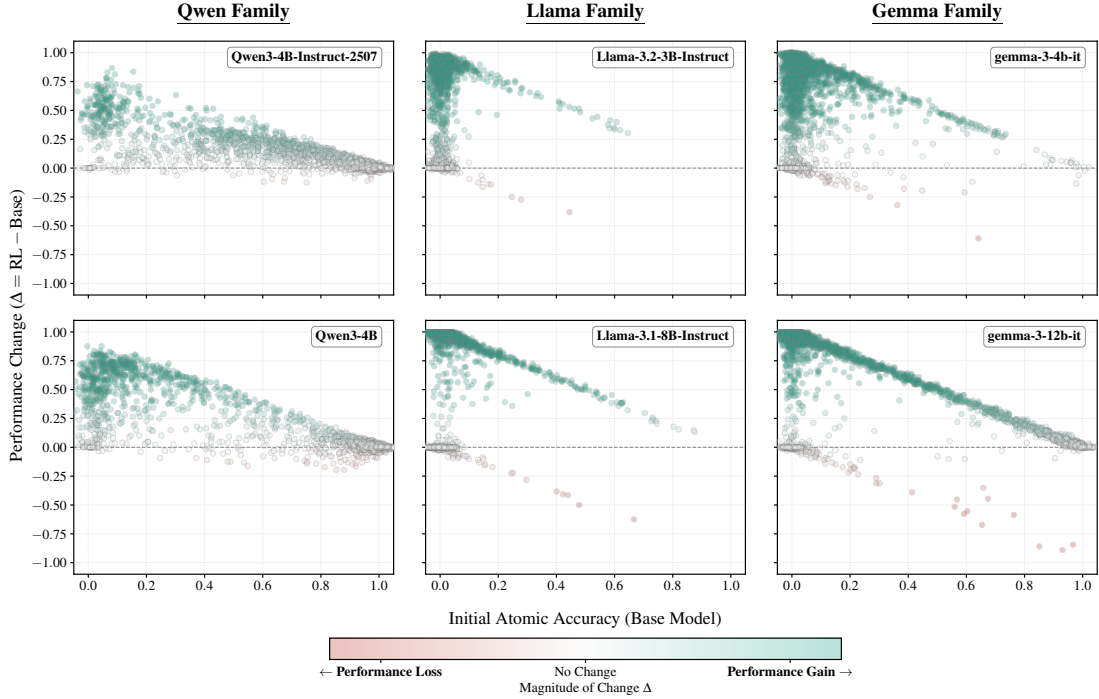


**Figure 6. Analysis of Atomic Performance Shifts.** Visualization of performance change ( $\Delta = \text{RL} - \text{Base}$ ) versus initial atomic accuracy. All model families achieve substantial performance gains across most atomic skills. However, Qwen demonstrates high robustness, achieving consistent gains with minimal regression in mastered skills. Conversely, Llama and Gemma exhibit a more extreme behavior. While they often achieve higher magnitude gains in weak areas, this often leads to a noticeable regression in previously acquired skills.

atomic steps and final results. The high correlation coefficients ( $\rho \in [0.69, 0.96]$ ) confirm that emergence is the direct mathematical consequence of pushing the joint process probability across the multiplicative barrier. Most critically, this indicates that complex capabilities introduced by RLVR are reducible to the mastery of constituent atomic tasks, suggesting a clear pathway for their acquisition.

#### 7.4. Capability Erosion under Atomic-Only RL

While RLVR fosters capability emergence, it can also induce performance erosion. As theorized in Section 5.3, its global optimization objective may sacrifice specialized skills to maximize aggregate rewards.

We examine the optimization dynamics in Figure 6 by plotting the performance change ( $\Delta$ ) against the initial accuracy for each atomic skill. As the initial mastery of a skill increases, the difficulty of further improvement rises, and the risk of regression emerges. However, the severity of this trade-off varies significantly.

**Llama & Gemma (High Severity).** These families show an extreme exchange. While they achieve substantial gains on initially weak skills, they pay a visible price in stability. The scatter plots reveal distinct clusters of negative values, indicating that the acquisition of new capabilities often comes

at the expense of eroding previously mastered skills.

**Qwen (Mitigated Severity).** Qwen manages this trade-off more effectively. While it also faces diminishing returns on high-accuracy skills, it avoids the catastrophic drops seen in others. This stability reflects that Qwen samples responses with stronger logical consistency. This internal consistency acts as a buffer, allowing Qwen to navigate the RLVR process and improve weak areas without largely sacrificing the integrity of its existing skills.

## 8. Conclusion

In this paper, we explain how RLVR enables the emergence of new capabilities. We reveal that instance-level correctness is the true driver of *Pass@k* performance. We identify the *Multiplicative Barrier* in complex reasoning, where the probability of success decays exponentially as reasoning chains lengthen. Then, we demonstrate that models overcome this by optimizing their existing capabilities. This optimization allows the model to discover valid reasoning paths that were previously inaccessible. Overall, our work contributes a novel explanation to the current discussion on emergent abilities in RLVR, suggesting that the iterative optimization of solvable problems enables models to develop the capabilities to tackle previously unsolvable scenarios.

---

## Impact Statement

This paper advances the understanding of how reinforcement learning facilitates complex reasoning in LLMs. By theoretically modeling the "Multiplicative Barrier" and clarifying the true drivers of performance beyond *Pass@k*, we provide actionable insights for improving model efficiency and correctness. These findings are instrumental for the research community to develop more effective training paradigms, ultimately leading to AI assistants that are capable of solving intricate problems with higher verifiable accuracy, benefiting fields ranging from automated coding to formal logic.

## References

Cheng, S., Yin, X., Zhou, R., Li, Y., Wang, X., Pan, L., Wang, W. Y., and Zhong, V. From atomic to composite: Reinforcement learning enables generalization in complementary reasoning, 2025. URL <https://arxiv.org/abs/2512.01970>.

Cui, G., Zhang, Y., Chen, J., Yuan, L., Wang, Z., Zuo, Y., Li, H., Fan, Y., Chen, H., Chen, W., Liu, Z., Peng, H., Bai, L., Ouyang, W., Cheng, Y., Zhou, B., and Ding, N. The entropy mechanism of reinforcement learning for reasoning language models, 2025. URL <https://arxiv.org/abs/2505.22617>.

DeepMind, G. Gemini 2.5: Pushing the frontier with advanced reasoning, multimodality, long context, and next generation agentic capabilities. *ArXiv*, abs/2507.06261, 2025.

DeepSeek-AI, Guo, D., Yang, D., Zhang, H., Song, J.-M., Zhang, R., Xu, R., Zhu, Q., Ma, S., Wang, P., Bi, X., Zhang, X., Yu, X., Wu, Y., Wu, Z. F., Gou, Z., Shao, Z., Li, Z., Gao, Z., Liu, A., Xue, B., Wang, B.-L., Wu, B., Feng, B., Lu, C., Zhao, C., Deng, C., Zhang, C., Ruan, C., Dai, D., Chen, D., Ji, D.-L., Li, E., Lin, F., Dai, F., Luo, F., Hao, G., Chen, G., Li, G., Zhang, H., Bao, H., Xu, H., Wang, H., Ding, H., Xin, H., Gao, H., Qu, H., Li, H., Guo, J., Li, J., Wang, J., Chen, J., Yuan, J., Qiu, J., Li, J., Cai, J., Ni, J., Liang, J., Chen, J., Dong, K., Hu, K., Gao, K., Guan, K., Huang, K., Yu, K., Wang, L., Zhang, L., Zhao, L., Wang, L., Zhang, L., Xu, L., Xia, L., Zhang, M., Zhang, M., Tang, M., Li, M., Wang, M., Li, M., Tian, N., Huang, P., Zhang, P., Wang, Q., Chen, Q., Du, Q., Ge, R., Zhang, R., Pan, R., Wang, R., Chen, R. J., Jin, R., Chen, R., Lu, S., Zhou, S., Chen, S., Ye, S., Wang, S., Yu, S., Zhou, S., Pan, S., Li, S. S., Zhou, S., Wu, S.-K., Yun, T., Pei, T., Sun, T., Wang, T., Zeng, W., Zhao, W., Liu, W., Liang, W., Gao, W., Yu, W.-X., Zhang, W., Xiao, W., An, W., Liu, X., Wang, X., aokang Chen, X., Nie, X., Cheng, X., Liu, X., Xie, X., Liu, X., Yang, X., Li, X., Su, X., Lin, X., Li, X. Q., Jin, X., Shen, X.-C., Chen, X., Sun, X., Wang, X., Song, X., Zhou, X., Wang, X., Shan, X., Li, Y. K., Wang, Y. Q., Wei, Y. X., Zhang, Y., Xu, Y., Li, Y., Zhao, Y., Sun, Y., Wang, Y., Yu, Y., Zhang, Y., Shi, Y., Xiong, Y., He, Y., Piao, Y., Wang, Y., Tan, Y., Ma, Y., Liu, Y., Guo, Y., Ou, Y., Wang, Y., Gong, Y., Zou, Y.-J., He, Y., Xiong, Y., Luo, Y.-W., mei You, Y., Liu, Y., Zhou, Y., Zhu, Y. X., Huang, Y., Li, Y., Zheng, Y., Zhu, Y., Ma, Y., Tang, Y., Zha, Y., Yan, Y., Ren, Z., Ren, Z., Sha, Z., Fu, Z., Xu, Z., Xie, Z., guo Zhang, Z., Hao, Z., Ma, Z., Yan, Z., Wu, Z., Gu, Z., Zhu, Z., Liu, Z., Li, Z.-A., Xie, Z., Song, Z., Pan, Z., Huang, Z., Xu, Z., Zhang, Z., and Zhang, Z. Deepseek-r1: Incentivizing reasoning capability in llms via reinforcement learning. *Nature*, 645, 2025.

---

Dziri, N., Lu, X., Sclar, M., Li, X. L., Jiang, L., Lin, B. Y., West, P., Bhagavatula, C., Bras, R. L., Hwang, J. D., Sanyal, S., Welleck, S., Ren, X., Ettinger, A., Harchaoui, Z., and Choi, Y. Faith and fate: Limits of transformers on compositionality, 2023. URL <https://arxiv.org/abs/2305.18654>.

Gandhi, K., Chakravarthy, A., Singh, A., nathan lile, and Goodman, N. D. Cognitive behaviors that enable self-improving reasoners, or, four habits of highly effective stars. *COLM*, 2025.

He, A., Fried, D., and Welleck, S. Rewarding the unlikely: Lifting grpco beyond distribution sharpening. *arXiv preprint arXiv:2506.02355*, 2025.

Jiang, Y., Li, Y., Chen, G., Liu, D., Cheng, Y., and Shao, J. Rethinking entropy regularization in large reasoning models, 2025. URL <https://arxiv.org/abs/2509.25133>.

Liu, Z., Chen, C., Li, W., Qi, P., Pang, T., Du, C., Lee, W. S., and Lin, M. Understanding r1-zero-like training: A critical perspective. *COLM*, 2025.

OpenAI. Openai o1 system card. *ArXiv*, 2024.

OpenAI, Akkaya, I., Andrychowicz, M., Chociej, M., Litwin, M., McGrew, B., Petron, A., Paino, A., Plappert, M., Powell, G., Ribas, R., Schneider, J., Tezak, N., Tworek, J., Welinder, P., Weng, L., Yuan, Q., Zaremba, W., and Zhang, L. Solving rubik’s cube with a robot hand. *CoRR*, abs/1910.07113, 2019. URL <https://arxiv.org/abs/1910.07113>.

Park, S., Kaur, S., and Arora, S. How does rl post-training induce skill composition? a case study on countdown, 2025. URL <https://arxiv.org/abs/2512.01775>.

Shao, Z., Wang, P., Zhu, Q., Xu, R., Song, J.-M., Zhang, M., Li, Y. K., Wu, Y., and Guo, D. Deepseekmath: Pushing the limits of mathematical reasoning in open language models. *ArXiv*, abs/2402.03300, 2024.

Wang, S., Yu, L., Gao, C., Zheng, C., Liu, S., Lu, R., Dang, K., Chen, X., Yang, J., Zhang, Z., et al. Beyond the 80/20 rule: High-entropy minority tokens drive effective reinforcement learning for llm reasoning. *arXiv preprint arXiv:2506.01939*, 2025.

Wei, J., Wang, X., Schuurmans, D., Bosma, M., Ichter, B., Xia, F., Chi, E., Le, Q., and Zhou, D. Chain-of-thought prompting elicits reasoning in large language models, 2023. URL <https://arxiv.org/abs/2201.11903>.

Wen, X., Liu, Z., Zheng, S., Xu, Z., Ye, S., Wu, Z., Liang, X., Wang, Y., Li, J., Miao, Z., et al. Reinforcement learning with verifiable rewards implicitly incentivizes correct reasoning in base llms. *arXiv preprint arXiv:2506.14245*, 2025.

Yan, J., Li, Y., Hu, Z., Wang, Z., Cui, G., Qu, X., Cheng, Y., and Zhang, Y. Learning to reason under off-policy guidance, 2025. URL <https://arxiv.org/abs/2504.14945>.

Yu, Q., Zhang, Z., Zhu, R., Yuan, Y., Zuo, X., Yue, Y., Dai, W., Fan, T., Liu, G., Liu, L., Liu, X., Lin, H., Lin, Z., Ma, B., Sheng, G., Tong, Y., Zhang, C., Zhang, M., Zhang, W., Zhu, H., Zhu, J., Chen, J., Chen, J., Wang, C., Yu, H., Song, Y., Wei, X., Zhou, H., Liu, J., Ma, W.-Y., Zhang, Y.-Q., Yan, L., Qiao, M., Wu, Y., and Wang, M. Dapo: An open-source llm reinforcement learning system at scale, 2025. URL <https://arxiv.org/abs/2503.14476>.

Yuan, L., Chen, W., Zhang, Y., Cui, G., Wang, H., You, Z., Ding, N., Liu, Z., Sun, M., and Peng, H. From  $f(x)$  and  $g(x)$  to  $f(g(x))$ : Llms learn new skills in rl by composing old ones, 2025. URL <https://arxiv.org/abs/2509.25123>.

Yue, Y., Chen, Z., Lu, R., Zhao, A., Wang, Z., Song, S., and Huang, G. Does reinforcement learning really incentivize reasoning capacity in llms beyond the base model? *ArXiv*, 2025.

Zhan, R., Li, Y., Wang, Z., Qu, X., Liu, D., Shao, J., Wong, D. F., and Cheng, Y. Exgrpo: Learning to reason from experience, 2025. URL <https://arxiv.org/abs/2510.02245>.

Zhao, R., Meterez, A., Kakade, S. M., Pehlevan, C., Jelassi, S., and Malach, E. Echo chamber: RL post-training amplifies behaviors learned in pretraining. *CoRR*, abs/2504.07912, 2025. doi: 10.48550/ARXIV.2504.07912. URL <https://doi.org/10.48550/arXiv.2504.07912>.

Zheng, C., Liu, S., Li, M., Chen, X.-H., Yu, B., Gao, C., Dang, K., Liu, Y., Men, R., Yang, A., Zhou, J., and Lin, J. Group sequence policy optimization, 2025. URL <https://arxiv.org/abs/2507.18071>.

Zhou, C., Liu, P., Xu, P., Iyer, S., Sun, J., Mao, Y., Ma, X., Efrat, A., Yu, P., Yu, L., Zhang, S., Ghosh, G., Lewis, M., Zettlemoyer, L., and Levy, O. Lima: Less is more for alignment, 2023. URL <https://arxiv.org/abs/2305.11206>.

Zhu, X., Xia, M., Wei, Z., Chen, W.-L., Chen, D., and Meng, Y. The surprising effectiveness of negative reinforcement in llm reasoning. *arXiv preprint arXiv:2506.01347*, 2025.

---

## A. Algebrarium Framework

To rigorously evaluate the symbolic reasoning capabilities of Large Language Models (LLMs) while mitigating the risks of data contamination, we developed **Algebrarium**. Unlike standard benchmarks that rely on static datasets, which are susceptible to memorization during pre-training, Algebrarium serves as a framework for the **procedural generation of synthetic algebraic tasks**. By constructing data dynamically based on arbitrary, user-defined mathematical structures, it establishes a hermetic evaluation environment where models must rely on on-the-fly reasoning rather than retrieval.

The core philosophy of Algebrarium lies in the decoupling of *abstract mathematical definition* from *concrete task generation*. This approach facilitates the creation of infinite variations of reasoning problems derived from a single logical core. The framework adheres to three fundamental principles:

**1. Arbitrary Algebraic Structures** Algebrarium treats algebra as a formal system defined by a tuple  $(S, \Sigma, \mathcal{A})$ , where  $S$  denotes a carrier set (finite or infinite),  $\Sigma$  represents a signature of operations with defined arities and precedence, and  $\mathcal{A}$  constitutes the axioms or computational rules governing interaction. Crucially, these structures are defined declaratively. This design allows the framework to generate tasks for standard structures, such as modular arithmetic or non-abelian groups, as well as entirely novel and custom-defined logical systems that the model has never encountered. Consequently, this enforces genuine zero-shot reasoning.

**2. Procedural Task Construction** Rather than retrieving pre-existing questions, the framework constructs reasoning tasks algorithmically. A generation engine instantiates specific algebraic instances and produces symbolic artifacts, such as expression trees or equations, to ensure that every sample is unique. This pipeline includes mechanisms for:

- **Controllable Complexity:** Parameters including recursion depth, expression length, and the cardinality of the underlying set can be adjusted to create a smooth difficulty gradient.
- **Diverse Task Types:** The engine supports various symbolic tasks, ranging from forward evaluation, such as reducing an expression  $a \circ b \circ c$  to a single element, to inverse reasoning, which involves solving equations like  $a \circ x = b$  or systems of group equations.

**3. Verifiable Ground Truth** Since the data is generated from formal logic rules, the “ground truth” is deterministic and mathematically verifiable. This characteristic allows for exact-match evaluation of the model’s outputs and enables the automatic generation of step-by-step Chain-of-Thought (CoT) traces for fine-tuning or interpretability studies.

## B. Implementation Details and Training Dynamics

### B.1. Base Models and Infrastructure

We evaluate a comprehensive suite of base models to ensure the generalizability of our findings. Our experiments cover three major model families:

- **Qwen3:** Qwen3-4B, and Qwen3-4B-Instruct.
- **Llama-3.1:** Llama-3.1-8B-Instruct and Llama-3.1-3B-Instruct.
- **Gemma-3:** gemma-3-4b-it and gemma-3-12b-it.

All models are trained using the `ver1` framework. We utilize `vLLM` for efficient rollout generation, employing Tensor Parallelism ( $TP = 2$ ) to handle the memory requirements of long-context reasoning up to 8,192 tokens.

### B.2. Hyperparameter Configuration

For all experiments, we employ Group Relative Policy Optimization (GRPO) using the AdamW optimizer with a learning rate of  $1 \times 10^{-6}$  over 100 optimization steps. The training is conducted with a global batch size of 128, a mini-batch size of 8, and a group size ( $G$ ) of 8, with gradient accumulation enabled. We set the maximum prompt and response lengths to 1,024 and 8,192 tokens, respectively. Regarding the RL objective, we monitor the KL divergence with a penalty coefficient  $\beta = 0.001$ , though the KL loss is not included in the optimization objective. Additionally, advantage normalization is disabled during training.

### B.3. Training Dynamics

We analyze the training stability and performance progression throughout the 100 optimization steps. As illustrated in Figure 7, we monitor two key metrics across the Qwen, Llama, and Gemma model families:

- **Critic Reward (Top Row):** The trajectory of the mean reward (Pass@1) starts near zero and exhibits a sharp increase before converging, indicating the models are effectively learning the target objective.
- **Actor Entropy (Bottom Row):** The policy entropy decreases rapidly during the initial phase and stabilizes as training progresses, reflecting the increasing confidence of the policy distribution.

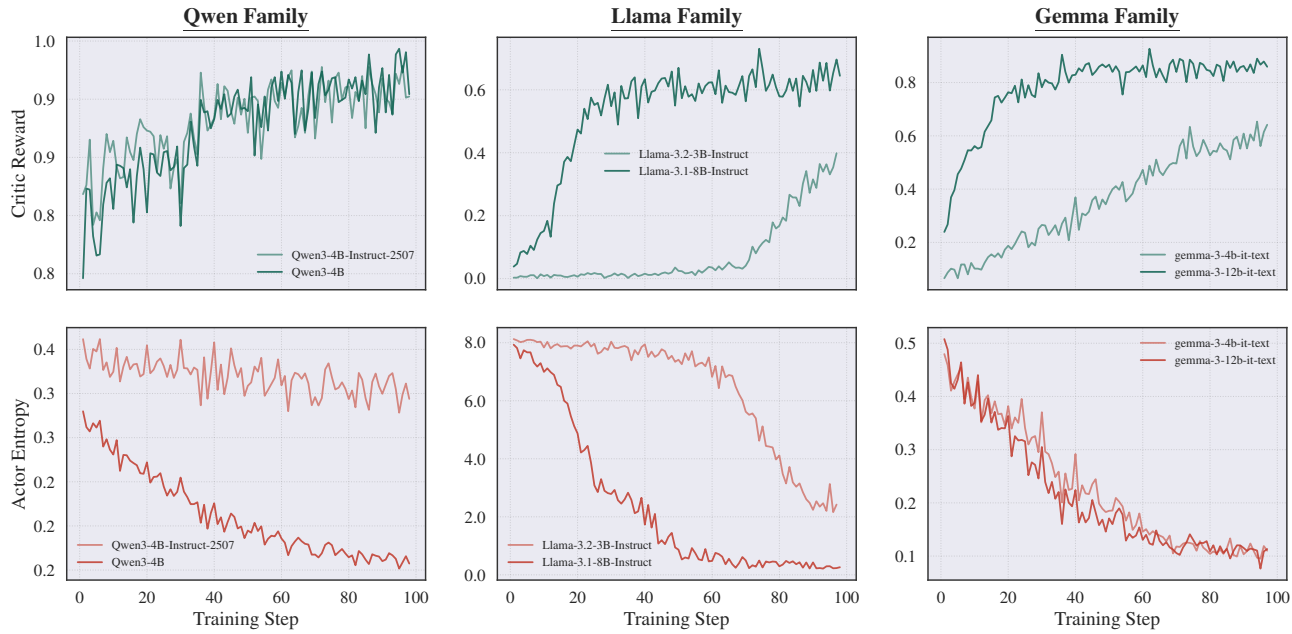


**Figure 7. Training Dynamics across Model Families.** The top row displays the evolution of Critic Reward, while the bottom row illustrates the Actor Entropy over 100 training steps. The results demonstrate consistent convergence behaviors across Qwen, Llama, and Gemma families.

## C. Domain Specifications and Operational Semantics

In this section, we provide the detailed formal specifications for the four algebraic systems employed in our experiments. Each system is constructed via the **Algebrarium** framework using distinct generative logic to cover different quadrants of group theory properties (Abelian vs. Non-Abelian, Finite vs. Infinite).

### C.1. Encrypted History Navigation (Infinite Abelian Group)

This domain models 1-dimensional navigation on an integer line, obfuscated by a substitution cipher. It tests the model's ability to perform arithmetic operations ( $\mathbb{Z}$ ) under symbolic encryption.

#### Representation

- **Base System:** Base-7.
- **Cipher Alphabet:** A bijective mapping  $\phi : \{0, \dots, 6\} \rightarrow \{a, \dots, g\}$  where  $0 \mapsto a, 1 \mapsto b, \dots, 6 \mapsto g$ .
- **Structure:** Elements are strings in the format  $\text{DIR}(\text{val})$ , where  $\text{DIR} \in \{\text{FWD}, \text{BACK}\}$  and  $\text{val}$  is a string of cipher characters representing a Base-7 magnitude.

---

**Operational Logic** Given two navigation steps  $S_1$  and  $S_2$ :

1. **Decryption:** The cipher string is decoded into a Base-10 integer  $N = \sum_{i=0}^{L-1} \phi^{-1}(c_i) \cdot 7^{(L-1-i)}$ .
2. **Signed Interpretation:** FWD implies  $+N$ , while BACK implies  $-N$ .
3. **Arithmetic Combination:** We compute  $R = N_1 + N_2$ .
4. **Re-encryption:** The result  $R$  is encoded back into the target format:
  - If  $R > 0$ , the direction is FWD.
  - If  $R < 0$ , the direction is BACK.
  - The absolute value  $|R|$  is converted to Base-7 and mapped via  $\phi$ .

**Example** Computing FWD (ad) + BACK (ef):

- $ad_7 \rightarrow 0 \cdot 7 + 3 = 3$ . Direction FWD  $\rightarrow +3$ .
- $ef_7 \rightarrow 4 \cdot 7 + 5 = 33$ . Direction BACK  $\rightarrow -33$ .
- Sum:  $3 + (-33) = -30$ .
- Result: Magnitude  $30 = 42_7 \rightarrow ec$ . Sign Negative  $\rightarrow$  BACK. Final: BACK (ec).

### C.2. Enigma 3-Rotor System (Finite Abelian Group)

This domain simulates the state of a simplified Enigma machine with three independent rotors. Mathematically, it represents the direct product group  $\mathbb{Z}_{26} \times \mathbb{Z}_{26} \times \mathbb{Z}_{26}$ .

#### Representation

- **State:** A comma-separated string  $R_1, R_2, R_3$  where each  $R_i \in \{A, \dots, Z\}$ .
- **Mapping:** Letters map to offsets  $0 \dots 25$  (A=0, B=1, ... Z=25).

**Operational Logic** The binary operation combines two states via component-wise addition modulo 26. Unlike a physical Enigma machine, there is no "carry" or stepping mechanism between rotors in this simplified algebraic model.

$$(r_1, r_2, r_3) \oplus (s_1, s_2, s_3) = ((r_1 + s_1) \bmod 26, (r_2 + s_2) \bmod 26, (r_3 + s_3) \bmod 26) \quad (10)$$

The inverse operation corresponds to negation modulo 26:  $\text{inv}(r) = (26 - r) \pmod{26}$ .

**Example** Computing A, C, Z  $\oplus$  B, B, C:

- Rotor 1:  $A(0) + B(1) = 1 \rightarrow B$
- Rotor 2:  $C(2) + B(1) = 3 \rightarrow D$
- Rotor 3:  $Z(25) + C(2) = 27 \equiv 1 \pmod{26} \rightarrow B$
- Result: B, D, B

### C.3. Knitting Instruction System (Infinite Non-Abelian Group)

This domain models a Free Group generated by two elements. It represents sequences of reversible actions where order matters and adjacent inverses cancel.

---

## Representation

- **Alphabet:**  $\Sigma = \{k, p, K, P\}$ .
- **Semantics:**  $k$  (knit),  $p$  (purl). Capital letters represent inverses:  $K = k^{-1}$  (un-knit),  $P = p^{-1}$  (un-purl).
- **Identity:** The empty string  $\epsilon$ .

**Operational Logic** The operation is string concatenation followed by recursive reduction. The reduction rule is defined by the cancellation of adjacent inverse pairs:

$$xx^{-1} \rightarrow \epsilon \quad \text{and} \quad x^{-1}x \rightarrow \epsilon \quad (11)$$

Specifically, the pairs  $(k, K)$  and  $(p, P)$  annihilate each other. This process repeats until the string is in its irreducible canonical form.

**Example** Computing  $kp \gg PK$ :

1. Concatenate:  $kpPK$
2. Inner Cancellation: The adjacent pair  $p, P$  cancels.  $k(pP)K \rightarrow kK$ .
3. Secondary Cancellation: The adjacent pair  $k, K$  cancels.  $kK \rightarrow \epsilon$ .
4. Result: Empty string (Identity).

## C.4. Rubik's Cube Sequence System (Finite Non-Abelian Group)

This domain models the algebra of face rotations on a  $3 \times 3 \times 3$  cube. It enforces strict canonicalization rules involving commutation and modulo arithmetic, representing a quotient of a free group.

## Representation

- **Moves:**  $F \in \{R, L, U, D, F, B\}$  representing face turns.
- **Modifiers:** None ( $90^\circ$  clockwise),  $\#$  ( $90^\circ$  counter-clockwise/prime), 2 ( $180^\circ$ ).
- **Sequence:** A space-separated list of moves (e.g.,  $R \ U \ R\#$ ).

**Operational Logic** Operations are defined by sequence concatenation followed by reduction to a unique **Canonical Form**. Three specific rules are applied iteratively:

1. **Inverse Cancellation:** Moves followed by their inverse are removed (e.g.,  $RR\# \rightarrow \epsilon$ ).
2. **Face Consolidation (Mod 4):** Consecutive moves of the same face are summed modulo 4.
  - Example:  $R \cdot R2 \rightarrow R3 \equiv R\#$  (since  $1 + 2 = 3 \equiv -1$ ).
  - Example:  $R \cdot R \cdot R \cdot R \rightarrow R4 \equiv \epsilon$ .
3. **Commutative Reordering:** While the group is generally non-abelian, opposite faces commute (e.g.,  $RL = LR$ ). To ensure a unique representation, we enforce a lexicographical priority:
  - $R$  precedes  $L$ ;  $U$  precedes  $D$ ;  $F$  precedes  $B$ .
  - Example: A sequence input as  $L \ R$  is automatically rewritten to  $R \ L$ .

---

**Example** Solving equation  $X = \text{inv}(R \ U) \cdot R \ U \ R\#$ :

1. Invert  $R \ U \rightarrow U\# \ R\#$ .
2. Concatenate:  $U\# \ R\# \ R \ U \ R\#$ .
3. Consolidate:  $R\#$  and  $R$  cancel. Sequence becomes  $U\# \ U \ R\#$ .
4. Consolidate:  $U\#$  and  $U$  cancel.
5. Result:  $R\#$ .